Peer-reviewed version available at Metals 2018, 8, 305; doi:10.3390/met8050305

Article

Microstructure and properties of 2219 aluminum alloy under compound technologies of friction-stir-welding, heat-treatment and electromagnetic forming

Zeyu Wang [1], Liang Huang [1,2,*], Jianjun Li [1], Xiaoxia Li [1], Hui Zhu [1], Fei Ma [3], Huijuan Ma [1] and Junjia Cui [2]

[1] State Key Laboratory of Materials Processing and Die & Mould Technology, School of Materials Science and Engineering, Huazhong University of Science and Technology, Wuhan 430074, China; raymond_w@hust.edu.cn (Z.W.); jianjun@mail.hust.edu.cn (J.L.); lixiaoxia@hust.edu.cn (X.L.); mahuijuan21@hust.edu.cn (H.M.); zhuhui@hust.edu.cn (H.Z.)

[2] State Key Laboratory of Advanced Design and Manufacturing for Vehicle Body, Hunan University, Changsha 410082, China; cuijunjia@hnu.edu.cn (J.C.)

[3] Changzheng Machinery Factory, China Aerospace Science and Technology Corporation, Chengdu 610100, China; mff126@126.com (F.M.)

* Correspondence: huangliang@hust.edu.cn; Tel.: +86-027-8754-3490

Abstract: Among all the processing technologies of heat-treatable aluminum alloys like 2219 aluminum alloy, using friction stir welding (FSW) as the joining technology and using electromagnetic forming (EMF) for plastic forming technology both have obvious advantages and successful applications. Therefore, there is a broad prospect for the compound technologies which can be used on the 2219 aluminum alloy to manufacture the large-scale thin-wall parts in the astronautic industry. The microstructure and mechanical properties of 2219 aluminum alloy under the process compounded of FSW, heat treatment, and EMF were investigated by means of tensile test, optical microscope (OM), and scanning electron microscope (SEM). The results show that the reduction of strength, which was caused during the FSW process, can be recovered effectively by the post-welding heat treatment composed of solid solution and aging, while the ductility was still reduced after heat treatment. Under the compound technology of FSW, heat treatment, and EMF, the forming limit of 2219 aluminum alloy decreased distinctly due to the poor ductility of the welding joint. A ribbon-pattern, which was formed due to the banded structure caused by FSW process, was found on the fracture surface of welded 2219 aluminum alloy after EMF treatment. During the EMF process, because of the effects of induced eddy current, a unique structure, which was manifested as a molted-surface appearance under the SEM observation, was formed as the material fractured.

Keywords: aluminum alloy; electromagnetic forming; friction stir welding; heat treatment; secondary phase

1. Introduction

With the characteristics of good weldability, corrosion stability and the superiorities in specific strength and thermal stability, 2219 aluminum alloy is a suitable material for manufacturing large-scale thin-wall parts in astronautic industry, such as the cryogenic fuel tank of launch vehicles[1-2]. The manufacturing process of 2219 aluminum alloy is composed of welding, heat treatment and plastic forming [3]. FSW can effectively minimize the thermal input and reduce the peak temperature compared with conventional welding technologies [4]. A welding joint with less welding defects and higher performance can be obtained through the solid bonding achieved by FSW [5]. Through a heat treatment composed of solid solution and aging, a dispersive distribution of secondary phase, which

Peer-reviewed version available at Metals 2018, 8, 305; doi:10.3390/met8050305

can bring an obvious improvement in the mechanical properties of 2219 aluminum alloy, can be achieved [6]. Meanwhile, as a high-velocity forming method, EMF can increase the forming limit of material and improve the performance of the workpieces compared with conventional quasi-static forming technologies [7-8]. Thus, in the field of astronautic industry, there is a broad prospect for the application of the compound technology of FSW, heat treatment and EMF in the manufacturing of large-scale thin-wall parts [9].

FSW technology has been widely applied in the manufacture for large-scale parts of aluminum alloy, and there are extensive researches for the influences of processing parameters and the plastic flow behavior during FSW treatment. After the FSW treatment, the microstructure and properties of welding joint on the butt welded 2219 aluminum alloy sheets are mainly affected by rotation speed, welding speed, pin geometry and the post-welding heat treatment[5; 10]. Because of the penetrating depth during FSW process, the surface material is extruded by the tool shoulder and flows downward under the stirring effect of pin. As the surface material flowing into the plastic zone, a banded structure named onion ring is formed under the interaction between the flowing material and in-situ material [11-12]. According to previous studies, through a proper post-weld annealing treatment, the mechanical properties of welded material can be recovered effectively, and even higher than the full-annealed base metal [13].

The studies of heat treatment on heat treatable aluminum alloys are mostly focused on the solid solution and aging treatment. A dispersively distributed secondary phase can be precipitated in the matrix of 2219 aluminum alloy during the heat treatment. The secondary phases, which is mainly composed of Al2Cu, play an important role in the aging strengthening of 2219 aluminum alloy [14]. The precipitating behavior of secondary phase can be greatly affected by the plastic deformation. With a proper deformation degree, a more dispersive distribution of secondary phase can be achieved, which can further improve the strength of 2219 aluminum alloy [15]. The plastic deformation also leads to an acceleration in the precipitating rate, and causes a changing in the optimum parameters of the aging treatment [16].

As for the EMF technology, it's a high-velocity forming technology, which is achieved by applying a pulse electromagnetic field on the formed material. The behavior of plastic deformation is affected by the coupled multi-field which is compounded of the electromagnetic field, induced eddy current and high-strain field [17-18], including the changing in the movement and pinning of dislocation and the distribution of low-angle grain boundary. A reduction of flow stress is observed while the plastic deformation is assistant with electricity [19], which is strongly associated with the temperature rising in the material caused by the Joule effect of electricity [20].

In a word, under the cooperative effects of the plastic flow in FSW, multi-times of thermal cycle and the coupled multi-physical field in EMF, the microstructure and mechanical properties of 2219 aluminum alloy change differently from conventional technologies during the compound technology of FSW, heat treatment and EMF, such as the expediting of precipitation because of FSW and the reduction of formability during EMF because of the existence of welding joint [9]. Thus, a study focused on this compound technology has a crucial significance for the application of 2219 aluminum alloy in astronautic industry.

In this work, the microstructure and the properties of 2219 aluminum alloy under different compound technologies of FSW and heat treatment are investigated through tensile test and SEM to study the interaction and the optimum combination of FSW and heat treatment. Then the samples of 2219 aluminum alloy under the optimum compound technology and the samples under the heat treatment are both processed by EMF treatment, and also the forming characteristics and the fracture appearance of 2219 aluminum alloy are discussed to study the influences of FSW treatment on the forming behavior of 2219 aluminum alloy during the EMF process.

2. Materials and Methods

The material used in this work was full-annealed 2219 Al alloy sheets with the thickness of 2 mm, and the chemical component of which is depicted in Table 1. By constituting the main secondary phase known as Al_2Cu in the matrix, Cu is the main strengthening element in the 2219 aluminum

Preprints (www.preprints.org) | NOT PEER-REVIEWED | Posted: 27 March 2018 doi:10.20944/preprints201803.0222.v1

Peer-reviewed version available at Metals 2018, 8, 305; doi:10.3390/met8050305

alloy [21], and Mn can increase the thermal stability of alloy by forming T phase. In FSW process, a tool with 10 mm shoulder diameter, 1.7 mm pin diameter and 1.7 mm pin length was used, and the schematic of FSW process is shown in Figure 1. The FSW was performed with a rotation speed of 1200 rpm and a welding speed of 200 mm/min which is perpendicular to the rolling direction. The shoulder penetrating depth was adjusted at 2 mm without tilting angle while the FSW was performing. The heat treatment includes a solid solution treatment of 535 ℃-40 min, water quenching and artificial aging of 180 ℃-6 h. A schematic of EMF process is shown in Figure 2 with the demonstration of samples which were used in the EMF process and the tensile test. Both of the samples were designed according to Chinese standard (GB/T 228-2002) and the main dimensions are illustrated in Figure 2. During EMF process, the capacitor was charged by the charging system, and a pulse electromagnetic field was generated by the discharging through the coil.

Table 1. Chemical composition of 2219 aluminum alloy (mass fraction, %)

Al	Cu	Mn	Ti	Zr	V
bal.	6.2	0.3	0.058	0.15	0.08

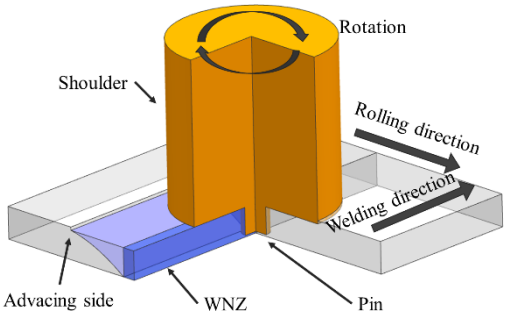

Figure 1. Schematic illustration of FSW process

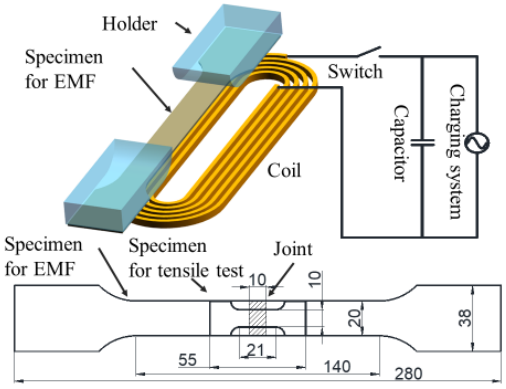

Figure 2. Schematic illustration of EMF process

The processing route is shown in Figure 3. Based on the heat treatment of solid solution and aging, the FSW was performed on the samples under different heat-treatment conditions including as-annealed, as-solid-solution and as-aged, to obtain various compound technologies of FSW and heat treatment. The microstructure and properties of these samples were compared by the means of tensile test, OM and SEM to study the interaction and the optimum compound technology of FSW and heat treatment. The EMF treatment was performed on the 2219 aluminum alloy samples, which were processed under the optimal compound technology of FSW and heat treatment, then the microstructure and properties were studied through forming characteristics and fracture morphology.

Peer-reviewed version available at Metals 2018, 8, 305; doi:10.3390/met8050305

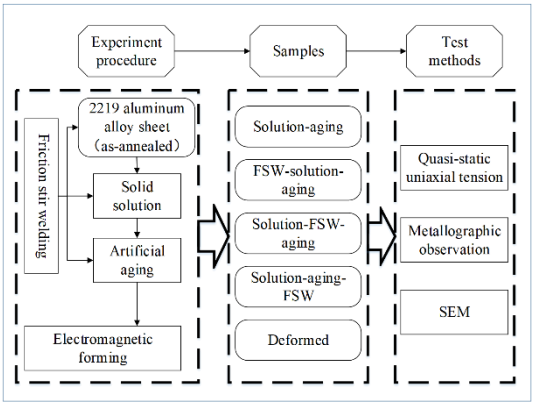

Figure 3. Schematic illustration of the processing route

The tensile test was performed on the AG-100kN testing machine with a tensile speed of 1 mm/min at room temperature. The samples were polished and etched with keller's reagent to revealed the microstructure for the OM observation on the welding joint, and the OM observation was performed on the VHX-1000C optical microscope. The fracture surface was observed using JSM-7600F FESEM.

3. Results and Discussion

3.1. Compound Technologies of FSW and Heat Treatment

3.1.1. Microstructure of Welding Joint

The cross-section structure of 2219 aluminum alloy FSW joint under the solution-aging-FSW technology is shown in Figure 4. According to Figure 4a, the cross-section of the 2219 aluminum alloy FSW joint is divided into four regions: the welding nugget zone (NZ), the thermos-mechanically affect zone (TMAZ), the heat-affect zone (HAZ) and the base metal. The NZ, which was directly affected by the pin and shoulder and experienced severe plastic flow during FSW process, is the central region of FSW joint with fine equiaxed grains. The TMAZ was affected by the plastic flow in NZ and the thermal cycle during FSW process. The grains in TMAZ were stretched along the flow direction. The HAZ has the similar structure with base metal but is slightly coarser as a result of the welding thermal cycle. The onion ring structure, which was formed due to the plastic flow during FSW process [11], is also observed in Figure 4a. The advanced side of the weld joint is shown in Figure 4b, it can be seen that the density of secondary particles in NZ is higher than other regions.

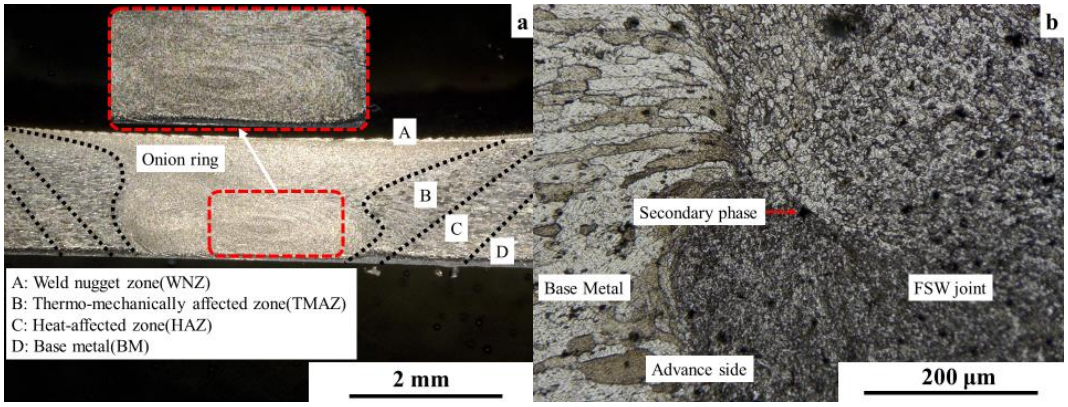

Figure 4. Schematic of FSW joint: (**a**) full view (**b**) partial enlarged view of advancing side

3.1.2. Mechanical Properties

The tensile test results of the 2219 aluminum alloy samples processed through solution-aging (base metal), FSW-solution-aging, solution-FSW-aging, and solution-aging-FSW are shown in Figure 5.

Based on the tensile strength shown in Figure 5, the base-metal samples and the FSW-solution-aging samples have a higher strength compared with the other two compound technologies. This is mainly due to the recovery and recrystallization reducing the negative effects of welding defects and plastic deformation caused by FSW, which is possible because of the high temperature during the solid solution treatment. The strength increase after aging treatment of solution-FSW-aging samples is not as high as the base-metal samples and the FSW-solution-aging samples. This can be attributed to the changes in the precipitation behavior of secondary phase caused by the FSW treatment. Especially the accumulation of dislocation can improve the precipitating rate during aging treatment. The localized deformation and thermal input in the welded region are harmful to the uniformity of the whole sample. As a result, the material of welding joint will reach the peak aging state sooner than base metal and will be overaged under the same aging treatment. The strength of the samples after solution-aging-FSW treatment is the lowest among three compound technologies. The welding defects and the accumulation of dislocations, which are caused by the FSW process and can't be recovered by heat treatment, are the main reason for the weakening of the welding joint.

Based on the elongation shown in Figure 5, the ductility of the samples under three compound technologies is obviously worse than base metal. According to the previous researches [12], the density of secondary phase is variable across the onion ring structure. In addition, the secondary phase can continually grow during aging treatment even the Cu element is no longer oversaturated [22]. The segregation and the coarsening of secondary phase are the main causes for the lower ductility of welded samples. For the FSW-solution-aging samples, the variation of the elongation and tensile strength during heat treatment is similar to the base-metal samples, which indicates that heat treatment has the similar effects on both the welded samples and the base metal. Meanwhile, the solution-FSW-aging samples show the worst ductility among all samples. This is because of the welding defects and overaging effect both caused by FSW. The elongation of solution-aging-FSW samples is similar to the FSW-solution-aging samples though there is a significant difference in the tensile strength of samples between these two technologies. This phenomenon indicates that the loss of strength due to FSW process can be recovered by solution-aging treatment, while the ductility is still reduced.

In conclusion, the welding defects and the accumulation of plastic deformation would cause a deterioration in mechanical properties after the FSW treatment. There will be a dramatic decrease in the ductility of 2219 aluminum alloy under the co-effect of FSW and heat treatment due to the interaction between severe plastic deformation and aging [23]. By comparing the tensile results which were processed under all the four technologies above, it's clear that the strength loss due to the FSW process can be largely recovered by solution-aging treatment, which is mainly because of the recovery and recrystallization in solid solution treatment.

Preprints (www.preprints.org) | NOT PEER-REVIEWED | Posted: 27 March 2018 doi:10.20944/preprints201803.0222.v1

Peer-reviewed version available at Metals 2018, 8, 305; doi:10.3390/met8050305

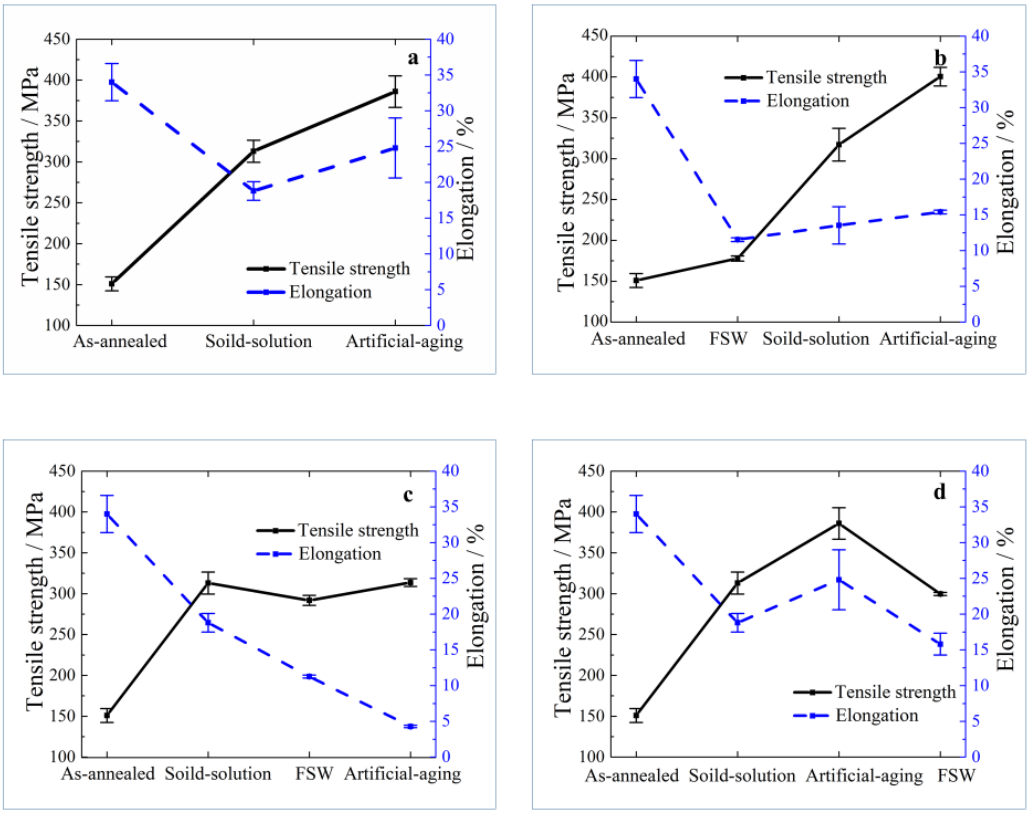

Figure 5. Comparison of quasi-static uniaxial tension result between base-metal sample and as-welded sample: (**a**) base metal (**b**) FSW-solution-aging (**c**)solution-FSW-aging (**d**) solution-aging-FSW

3.1.3 Fracture Appearance

The SEM observations of the fractures, which was formed during tensile test, are shown in Figure 6. The fracture of FSW-solution-aging sample shown in Figure 6b is a typical alloyed fracture appearance, which is a dispersive distribution of large-sized dimples surrounded by small-sized dimples. Secondary particles can be observed at the bottom of some dimples and the tearing ridge on the dimples is sharp. This is similar to the fracture appearance of base metal shown in Figure 6a. The fracture of the solution-FSW-aging sample shown in Figure 6c has a quasi-dissociation fracture appearance. The dimples are shallow and small, with the less sharp tearing ridge, which indicates a poor ductility of the 2219 aluminum alloy. The fracture appearance of the solution-aging-FSW sample shown in Figure 6d has the morphology characteristic of both FSW-solution-aging sample and solution-FSW-aging sample. The large-sized dimple found in Figure 6a and Figure 6b can′t be found on the fracture surface of the solution-aging-FSW sample, which leads to a more uniform size distribution of dimples. It has been known that the appearance of dimples is greatly affected by the secondary particles in the matrix [24], thus a conclusion is drawn: the size distribution of the secondary phase becomes more uniform after FSW process because of the fragmenting of large-sized particles caused by the severe plastic deformation. This distribution leads to the formation of fracture appearance shown in Figure 6d. For the fracture appearance of the solution-FSW-aging sample, the severe plastic deformation caused by FSW is a strong boost for precipitating rate during the aging processing. Thus, the aging treatment can significantly increase the negative effects of FSW on the materials′ mechanical properties, even caused the banded appearance on Figure 6c.

The size of dimples was measured by the linear intercept method, and the results are shown in Figure 6e. It's obvious that the FSW-solution-aging sample and base-metal sample have better ductility according to the size of dimples, and the solution-FSW-aging sample shows the worst ductility among all samples, which is consisted with the tensile test results.

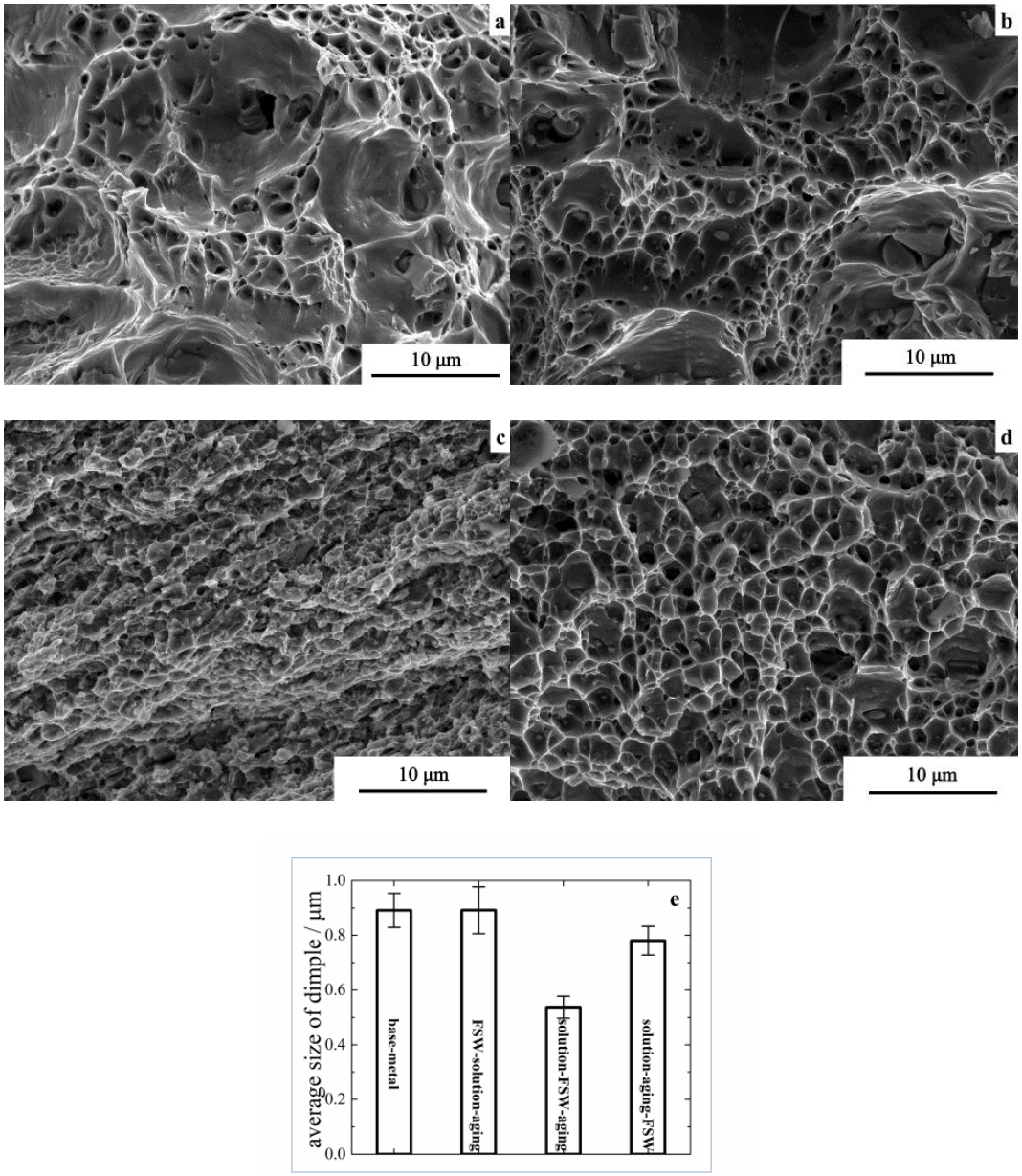

Figure 6. Schematic of fracture of 2219 aluminum alloy under different compound technology: (**a**) base metal (**b**) FSW-solution-aging (**c**) solution-FSW-aging (**d**) solution-aging-FSW (**e**) average size of dimple

3.2. EMF Treatment

3.2.1 Forming Characteristics

The EMF treatment was performed on the samples under solution-aging treatment and FSW-solution-aging treatment, which has showed the optimal properties of all three compound technologies. The results shown in Figure 7 indicate that welded samples tend to fracture at lower discharging voltage compared with the base-metal samples. The comparison of the forming height shows that the maximal strain of welded samples is significantly lower than base-metal samples. The fracture location on welded samples is around the middle of the welding joint where the NZ is located, while it's die corner on the base-metal samples where the stress concentration occurs.

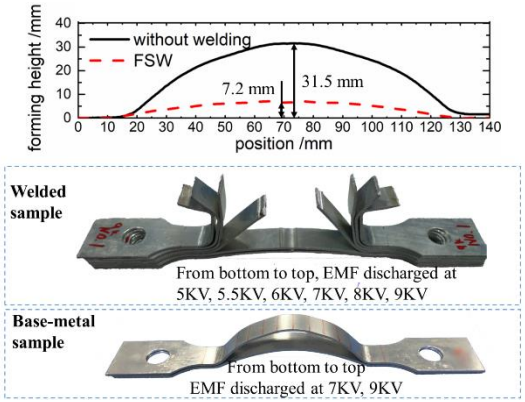

Figure 7. Comparison of EMF between base-metal sample and as-welded sample

3.2.2 Fracture Appearance

The fracture appearance of the welded sample and base-metal sample is shown in Figure 8. It's obvious that there are both bright silver region on the fracture surface. Under further observation which is performed by SEM and shown in Figure 8b and Figure 8f, this structure is large-scale surface with a melted appearance. Meanwhile, the fracture surface of friction-stir-welded samples has a layered structure which doesn't appear on the base-metal sample. A banded texture is also found on the fracture surface of the welded sample, and the further observations are shown in Figure 8c and Figure 8d.

Observation of Figure 8c indicates an alternative distribution of dimples in different size, there is also a texture of the holistic distribution of dimples which caused the banded texture on the fracture surface which can be attributed to the onion ring structure in the welding joint. The microstructure of welded material is various across the onion ring structure, such as the density of the secondary phase is different between the bright and dark layers in the onion structure. The variation of microstructure leads to a regular variation in the mechanical properties and cause the corresponding structure on the fracture surface.

The fracture surface shown in Figure 8d indicates a multi-fracture-type structure with few dimple structure, even though it's similar in macrostructure with the fracture appearance shown in Figure 8c. There are also brittle fracture appearances such as intergranular fracture besides the ductile fracture structure like dimples or sliding separation. The banded structure is mainly caused by the plastic flow during FSW process, and the multi-fracture-type structure can be attributed to two reasons: the lack of the driving force from welding shoulder causing a relatively weak region of welding joint, and the heat from the Joule effect of induced current causing a weakening of the grain boundaries.

As for the fracture structure of base-metal sample under EMF process, there is also multi-fracture-type structure as shown in Figure 8g and Figure 8h, but no banded structure appeared.

Peer-reviewed version available at Metals 2018, 8, 305; doi:10.3390/met8050305

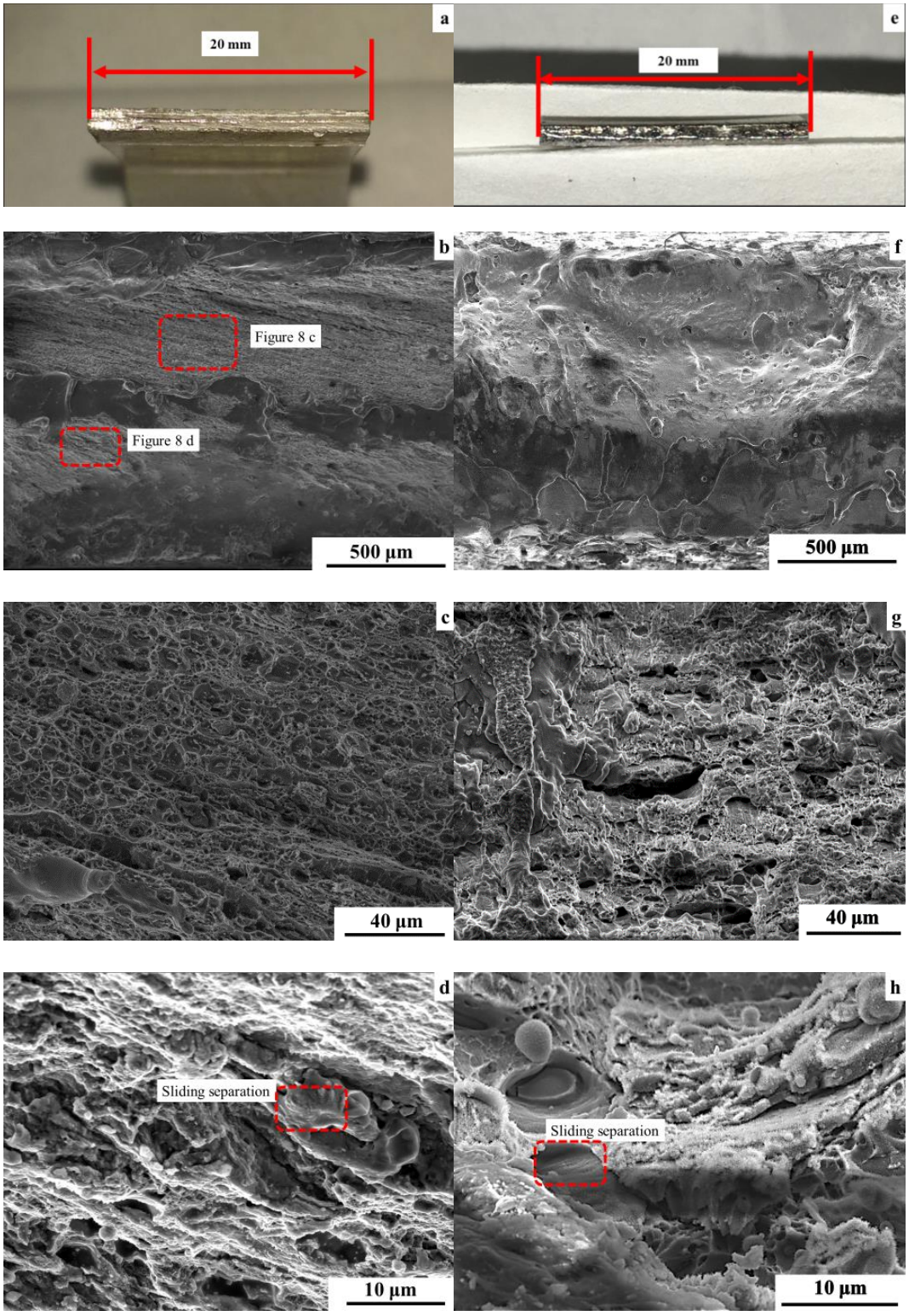

Figure 8. Fracture appearance of EMF samples: (**a**)–(**d**) as-welded sample (**e**)–(**h**) base-metal sample

Further observations of the large-scale surface with a melted appearance are shown in Figure 9. There is pit structure like dimples with sliding separation structure on the side wall appearing on the large-scale surface as shown in Figure 9b. Meanwhile, a structure of crack also found on the surface and observed in high magnification as shown in Figure 9c. It's easy to find a pattern of grain boundaries is showed around the crack, and the size of which is close to the size of the grains in the NZ which is around 5~10 μm.

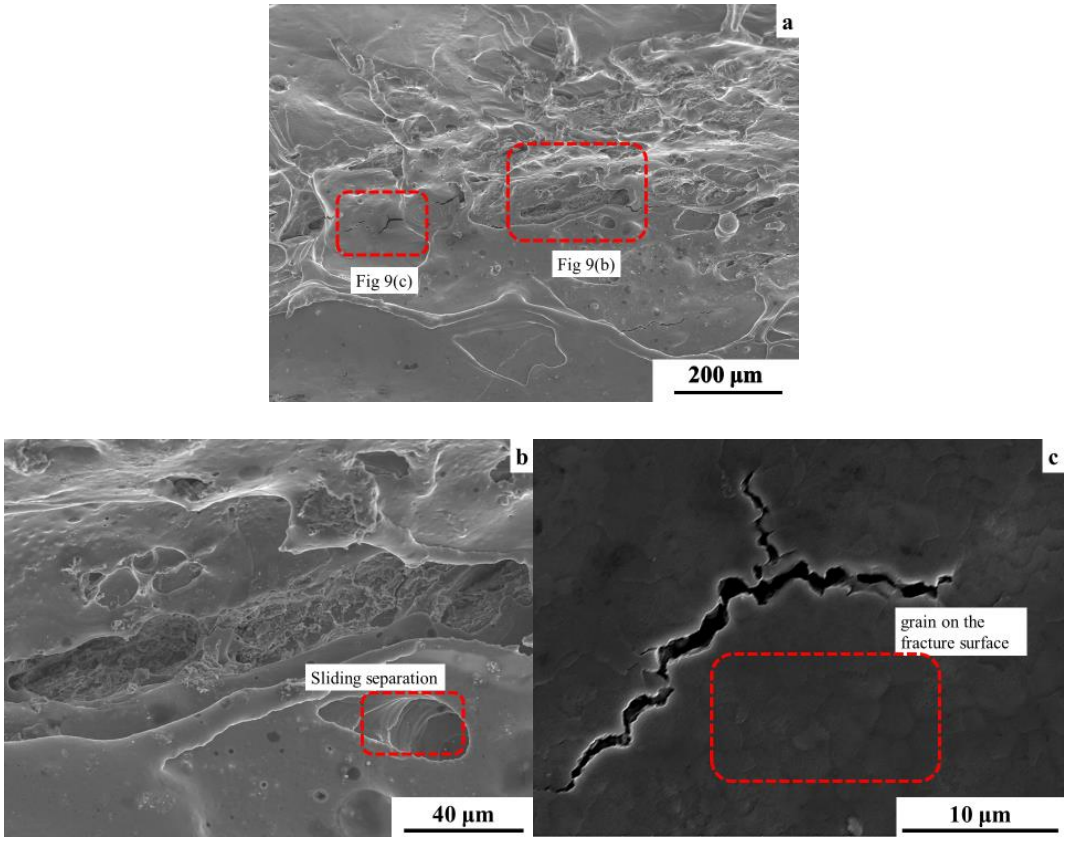

Figure 9. Appearance of flat fracture surface

In conclusion, EMF process is greatly affected by the FSW treatment:

FSW treatment causes a weakening in the properties of welded material because of welding defects such as segregation of secondary phase and the liquation cracking [25]. And the Joule effect of induced eddy current during EMF also bring down the ductility of 2219 aluminum alloy during EMF process. The microstructure variation across the onion ring structure, which was formed during FSW process, causes a variation of mechanical properties and leads to the banded structure on the fracture surface of electromagnetic-formed samples. Because only the upper layer of 2219 aluminum alloy can be affected by the friction of shoulder during single-shoulder FSW process, a weak region in the bottom of welding joint is produced. With the addition of skin effect of the induced eddy current during EMF process, the fracture type is various in different thickness of the sample.

A conclusion can be drawn on the formation of the large-scale surface: the welding defects and regional secondary phase segregation cause an increase in electrical resistance and led to a higher temperature rising under the Joule effect during EMF process. The strength of the welding joint was weakened under high temperature and an intergranular fracture was formed because of the weakened grain boundaries. When the samples fractured, a strong electric arc occurred which can be seen clearly during EMF process. The surface of fracture was partially melted under the effect of the arc, and the melted appearance is formed.

4. Conclusions

1. The effects of high temperature during heat treatment drive 2219 aluminum alloy to recovery and recrystallization, which is able to recover the strength reduced during FSW process, but the ductility remains the state of reduced after heat treatment. The performance of FSW after solid-solution treatment on 2219 aluminum alloy causes an overaging effect during subsequent aging treatment, and leads to a poor ductility.
2. The formability of welded samples under EMF is lower compared with base-metal samples because of the poor mechanical properties. The onion ring structure formed during FSW treatment causes a variation in both microstructure and properties of 2219 aluminum alloy, and leads to the banded structure on the fracture surface. A multi-fracture-type structure was generated due to the interaction of plastic flow caused by FSW and induced eddy current caused by EMF.
3. During EMF process, an intergranular fracture appearance was generatede because of the Joule effect of the induced eddy current, which also caused the electric arc leading to the melt of the fracture surface when the fracture occurred. The melted surface covered the original fracture appearance and formed the bright silver appearance on the fracture surface of 2219 aluminum alloy under EMF treatment.

Acknowledgments: This work was supported by the National Natural Science Foundation of China (Grant No. 51575206 and 51435007), the EU Marie Curie Actions-MatProFuture Project (Grant No. FP7-PEOPLE-2012-IRSES-318968), the Innovation Funds for Aerospace Science and Technology from China Aerospace Science and Technology Corporation (Grant No. CASC150704), the Open Funds from the State Key Laboratory of Advanced Design and Manufacturing for Vehicle Body (Grant No. 31615006), the Fundamental Research Funds for the Central University (Grant No. 2016YXZD055).

Author Contributions: Zeyu Wang, Liang Huang and Xiaoxia Li designed and performed the experiments; Zeyu Wang, Liang Huang and Huijuan Ma analyzed and discussed the data; Jianjun Li, Hui Zhu, Fei Ma and Junjian Cui provided guidance for this research; Zeyu Wang and Liang Huang wrote the paper;

Conflicts of Interest: The authors declare no conflict of interest.

References

1. Narayana, G. V., Sharma, V. M. J., Diwakar, V., Kumar, K. S. and Prasad, R. C., Fracture behaviour of aluminium alloy 2219 – T87 welded plates, *Sci. Technol. Weld. Joi.*, **2013**, 9,121-130.
2. Gupta, R. K., Panda, R., Mukhopadhyay, A. K., Kumar, V. A. and Sankaravelayutham, P., Study of Aluminum Alloy AA2219 After Heat Treatment, *Met. Sci. Heat Treat.+*, **2015**, 57,350-353.
3. Klett, A., Hegels, J., Bartesch, G., Glaser, U. and Mold, E., Spinforming of Friction Stir Welded AA2219 Circular Blanks for ARIANE 5 Main Stage Tank Bulkheads, *DVS BERICHTE*, **2004**, 229,90-94.
4. Regensburg, A., Schürer, R., Weigl, M. and Bergmann, J., Influence of Pin Length and Electrochemical Platings on the Mechanical Strength and Macroscopic Defect Formation in Stationary Shoulder Friction Stir Welding of Aluminium to Copper, *Metals*, **2018**, 8,85.
5. Zhang, Z., Xiao, B. L. and Ma, Z. Y., Effect of welding parameters on microstructure and mechanical properties of friction stir welded 2219Al-T6 joints, *J. Mater. Sci.*, **2012**, 47,4075-4086.
6. Son, S. K., Takeda, M., Mitome, M., Bando, Y. and Endo, T., Precipitation behavior of an Al – Cu alloy during isothermal aging at low temperatures, *Mater. Lett.*, **2005**, 59,629-632.
7. Seth, M., Vohnout, V. J. and Daehn, G. S., Formability of steel sheet in high velocity impact, *J. Mater. Process. Tech.*, **2005**, 168,390-400.
8. Psyk, V., Risch, D., Kinsey, B. L., Tekkaya, A. E. and Kleiner, M., Electromagnetic forming—A review, *J. Mater. Process. Tech.*, **2011**, 211,787-829.
9. Zhu, H., Huang, L., Li, J., Li, X. and Ma, H., Strengthening mechanism in laser-welded 2219 aluminium alloy under the cooperative effects of aging treatment and pulsed electromagnetic loadings, *Materials Science and Engineering: A*, **2018**, 714,124-139.
10. Mohammadi-pour, M., Khodabandeh, A., Mohammadi-pour, S. and Paidar, M., Microstructure and mechanical properties of joints welded by friction-stir welding in aluminum alloy 7075-T6 plates for aerospace application, *Rare Metals*, **2016**, 1-9.
11. Hamilton, C., Dymek, S. and Blicharski, M., A model of material flow during friction stir welding, *Mater. Charact.*, **2008**, 59,1206-1214.
12. Krishnan, K. N., On the formation of onion rings in friction stir welds, *Materials Science and Engineering: A*, **2002**, 327,246-251.
13. Chu, G., Sun, L., Lin, C. and Lin, Y., Effect of Local Post Weld Heat Treatment on Tensile Properties in Friction Stir Welded 2219-O Al Alloy, *J. Mater. Eng. Perform.*, **2017**, 26,5425-5431.
14. Wang, S. C. and Starink, M. J., Precipitates and intermetallic phases in precipitation hardening Al-Cu-Mg-(Li) based alloys, *Int. Mater. Rev.*, **2005**, 50,193-215.
15. AN, L., CAI, Y., LIU, W., YUAN, S. and ZHU, S., Effect of pre-deformation on microstructure and mechanical properties of 2219 aluminum alloy sheet by thermomechanical treatment, *T. Nonferr. Metal. Soc.*, **2012**, 22,s370-s375.
16. NING, A., LIU, Z. and ZENG, S., Effect of large cold deformation after solution treatment on precipitation characteristic and deformation strengthening of 2024 and 7A04 aluminum alloys, *T. Nonferr. Metal. Soc.*, **2006**, 16,1341-1347.
17. Tan, J., Zhan, M. and Liu, S., Guideline for Forming Stiffened Panels by Using the Electromagnetic Forces, *Metals*, **2016**, 6,267.
18. Liu, Z., Fan, T. and Hu, H., Possible Mechanism of Plasticity Influenced by Magnetic Field, *CHIN.PHYS.LETT.*, **2006**, 23,175-177.
19. Ruszkiewicz, B. J., Grimm, T., Ragai, I., Mears, L. and Roth, J. T., A Review of Electrically-Assisted Manufacturing with Emphasis on Modeling and Understanding of the Electroplastic Effect, *Journal of Manufacturing Science & Engineering*, **2017**, 139,1-15.
20. Kaltenboeck, G., Demetriou, M. D., Roberts, S. and Johnson, W. L., Shaping metallic glasses by electromagnetic pulsing, *Nat. Commun.*, **2016**, 7,10576.
21. Ringer, S. P. and Hono, K., Microstructural Evolution and Age Hardening in Aluminium Alloys: Atom Probe Field-Ion Microscopy and Transmission Electron Microscopy Studies, *Mater. Charact.*, **2000**, 44,101-131.
22. Liu, G. and Sun, J., A Model for Age Strengthening of plate-like-precipitate-containing Al Alloys, *The Chinese Journal of Nonferrous Metals*, **2001**, 337-347. (in Chinese)
23. NING, A., LIU, Z. and ZENG, S., Effect of large cold deformation on characteristics of age-strengthening of 2024 aluminum alloys, *T. Nonferr. Metal. Soc.*, **2006**, 16,1121-1128.

24. Mittra, J., Banerjee, S., Tewari, R. and Dey, G. K., Fracture behavior of Alloy 625 with different precipitate microstructures, *Materials Science and Engineering: A*, **2013**, 574,86-93.
25. C, H. and S, K., Partially Melted Zone in Aluminum Welds — Liquation Mechanism and Directional Solidification, *WELDING JOURNAL-NEW YORK*, **2000**, 79,113.